ELSEVIER

Chemical Physics 265 (2001) 177–191

Chemical Physics

www.elsevier.nl/locate/chemphys

The correlation between the phase transitions and vibrational properties by Raman spectroscopy: liquid–solid β and solid β–solid α acetonitrile transitions

H. Abramczyk *, K. Paradowska-Moszkowska

Department of Chemistry, Institute of Applied Radiation Chemistry, Technical University, 93-590 Łódź, Wróblewskego Street 15, Poland

Received 16 October 2000; in final form 30 January 2001

Abstract

Raman spectra of the internal vibrational modes: $\nu_5(E)$, $\nu_1(A_1)$, $\nu_2(A_1)$, $\nu_6(E)$, $\nu_3(A_1)$, $\nu_4(A_1)$, $\nu_8(E)$ and the external modes in the region of 15–200 cm^{-1} of acetonitrile have been recorded in the 77–293 K range at the atmospheric pressure. One of the goals of the paper is to develop a correlation between the liquid–solid β and solid β–solid α transitions of acetonitrile on the one hand and the vibrational properties of the internal and external lattice modes on the other. The Raman spectra of acetonitrile in the region of the phase transitions have been recorded for the first time. © 2001 Published by Elsevier Science B.V.

1. Introduction

Numerous theoretical, experimental and simulation studies of acetonitrile in the gas phase [1,2], liquid phase [3–16], clusters [17,18] and solid phases [19–31] have focused on approaches to understand interactions, crystals structure, mechanisms of the solvent–reactant coupling, and solvation dynamics.

All investigations in the liquid phase lend support to highly associated structure with anti-parallel arrangement of neighbouring molecules and microscopic structure determined by the competition between the repulsive and attractive forces arising most likely from dispersive and dipolar interactions.

Solid acetonitrile exists in two stable phases. The β phase is stable between the melting point (229 K) and the temperature of the solid–solid ($\beta \rightarrow \alpha$) transition at approximately 211 K [24], 216.9 K [29], 217 K [26] according to different sources. The α phase is stable below the $\beta \rightarrow \alpha$ transition temperature.

Although quite a number of studies have addressed the questions of crystal structure of the β and α phases as well as supercooled β acetonitrile and the molecular mechanisms leading to the $\beta \rightarrow \alpha$ transitions, the answers are as yet incomplete. Moreover, much confusion in literature exists on the nomenclature of the acetonitrile phases. Some papers called the stable β and α phases as the Form II, the supercooled β phase as the Form I [20,21]. The more recent papers [24–27] reversed the names for β and α phases in comparison with

* Corresponding author. Fax: +48-42-360246/+48-42-6313188.

E-mail address: abramczy@mitr.p.lodz.pl (H. Abramczyk).

0301-0104/01/$ - see front matter © 2001 Published by Elsevier Science B.V.
PII: S0301-0104(01)00271-3

those in Ref. [19], the first one in which the crystal structure of α acetonitrile has been determined. The results obtained in Refs. [19,24,28] from crystallographic analysis suggested that the phase transition β → α is accompanied by the dramatic volume expansion of the unit cell from 267 Å^3 (β) [28] or 271 Å^3 [24] to 455 Å^3 (α) [19]. In contrast to those studies, a small volume changes: 271 Å^3 [24] → 246.95 Å^3 [26], 271 Å^3 [24] → 257.73 Å^3 [25] have been reported in recent crystallographic papers. However, the results of those papers suggested dramatic changes in the orientation of permanent dipoles of the acetonitrile molecules relative to the crystallographic axes of the unit cell during the phase transition β → α, which lead to a structure of α acetonitrile with a macroscopic polarisation along the crystallographic axis *c* in the orthorhombic $Cmc2_1$ unit cell. Early papers suggested axial anti-parallel alignment for the β phase [19,30]. Recent crystallographic studies and some previous ones suggest the anti-parallel alignment for both β and α phases [21] or anti-parallel for the β phase [24] and parallel for the α phase [26] with the molecular axis C_3 of acetonitrile tilted with respect to the crystallographic axis *c*. The significant symmetry change is suggested to occur at the β → α transition from the monoclinic $P2_1/c$ space group and four molecules in the unit cell located at C_1 sites [24] to the orthorhombic Pbam space group with eight molecules in the unit cell located at C_s sites [19], or four molecules at C_s sites in the orthorhombic $Cmc2_1$ unit cells [25,26]. The recent X-ray data prove the occurrence of a $P2_1/c$ monoclinic cell with four molecules with anti-parallel alignment of the dipoles for the β phase and an orthorhombic $Cmc2_1$ unit cell with four molecules with parallel alignment of the dipoles for the α phase [31]. Although this brief review certainly does not provide a current status report on the solid phases of acetonitrile, it points out those features that are not completely convincing and illustrates that a more complete picture of the structure and dynamics as well as detailed molecular mechanisms for the phase transitions in acetonitrile would be needed.

Raman spectra of acetonitrile and deuterated acetonitrile for the internal vibrational modes $\nu_5(E)$, $\nu_1(A_1)$, $\nu_6(E)$, $\nu_2(A_1)$, $\nu_3(A_1)$, $\nu_4(A_1)$, $\nu_8(E)$ and the external modes in the region of 15–200 cm^{-1} have been presented as a function of temperature in the range of 77–293 K. We will show that the liquid → solid β phase and solid β → solid α transitions are accompanied by marked changes in the Raman spectra. We will show that the low temperature Raman spectroscopy provides useful information about the nature of the phase transitions at the molecular level, and in some favourable cases may provide valuable information about the crystal space group, the molecular site group as well as the factor group.

The aim of the present study is to obtain information about the nature of the β → α transition in acetonitrile and to give a contribution to understanding the correlation between the mechanism of the phase transitions and vibrational properties of the internal and external modes in the lattice region.

This paper is organised as follows. Experimental procedures to generate and measure β, α, and β supercooled phases of acetonitrile are described in Section 2. In Section 3 we present and discuss results in the light of the current understanding of molecular mechanisms and we attempt to provide a molecular level picture of the β → α phase transition of acetonitrile. Finally, in Section 4 we conclude by summarising our main results.

2. Experimental procedure

Spectrograde acetonitrile was purchased from Aldrich. Raman spectra were recorded with Ramanor U 1000 (Jobin Yvon) and Spectra physics 2017 – 04S argon ion laser operating at 514 nm. The internal vibrational modes of acetonitrile $\nu_5(E)$, $\nu_1(A_1)$, $\nu_6(E)$, $\nu_2(A_1)$, $\nu_3(A_1)$, $\nu_7(E)$, $\nu_4(A_1)$, $\nu_8(E)$ and the external modes in the lattice region 15–200 cm^{-1} have been recorded as a function of temperature in the range of 293–77 K. The spectral slit width was 1.3 cm^{-1}, which corresponds to 200 μm mechanical slit of the spectrometer. The polarisation analyzer and the wave plate $\lambda/4$ were used to select VV and VH components. The interference filter was used to purify the laser line by removing additional natural emission lines that interfere with the Raman lines, especially in the

case of solid samples. Solid acetonitrile exists in two stable phases β and α. The Raman spectra of acetonitrile were recorded in commercial glass ampoules mounted in a special cell arrangement in the cryostat (Oxford Instruments Limited). The samples were introduced as a liquid and were cooled in the cryostat equipped with a heater and thermocouples for temperature monitoring. The local temperature was checked by the Stokes/anti-Stokes intensity ratio. The difference between these methods never exceeded 1–2 K. Cooling of the sample was achieved by the use of 50 l liquid-nitrogen Dewar which supplied a small stream of liquid nitrogen through a vacuum jacketed tube to the cryostat coat. It was found that the cooling rate of 0.5°C/min was sufficient to insure the generation of the stable β acetonitrile in the liquid–solid β acetonitrile transition and the complete conversion of β acetonitrile into stable α acetonitrile at $\beta \rightarrow \alpha$ transition. During cooling the sample in the cryostat was exposed to the incident argon laser beam. Differential scanning calorimetry (DSC) method has been used to monitor the phase transitions. The DSC traces were measured during the heating of the frozen sample as well as the cooling of the liquid sample at normal pressure with Netzsch DSC 200 instrument in ampoules of 80 mg.

3. Results and discussion

Figs. 1–7 show the Raman (VV components) band shapes of the $\nu_5(E)$ asymmetric C–H stretching, $\nu_1(A_1)$ symmetric C–H stretching, ν_2 (A_1) symmetric C≡N stretching, $\nu_6(E)$ asymmetric CH_3 deformation, $\nu_3(A_1)$ symmetric CH_3 deformation, $\nu_4(A_1)$ symmetric C–C stretching and ν_8 (E) C–C≡N bending of acetonitrile, respectively. The assignments were taken from the Ref. [32] although there is some confusion regarding the assignments of the modes in the region around 1400 cm^{-1} [19,20] due to Fermi resonances. We can see remarkable red shifts for ν_5, ν_1, ν_2, ν_3 modes, blue shifts for ν_6, ν_8 modes, and the lack of considerable changes for the ν_4 mode with decreasing temperature. The trend of the changes is the same as observed in the gas–liquid phase transition [19]. Some of the bands show a slight asymmetry on red (ν_2) or blue (ν_4) side. The asymmetry disappears with decreasing temperature as it is illustrated in Figs. 5 and 6 conclusively demonstrating that it comes from hot bands and should not be assigned to dimers or clusters. As one see from Figs. 1–7 the broad, structureless bands observed in the liquid phase between 293 and 229 K show a dramatic change when the temperature goes below the freezing point temperature

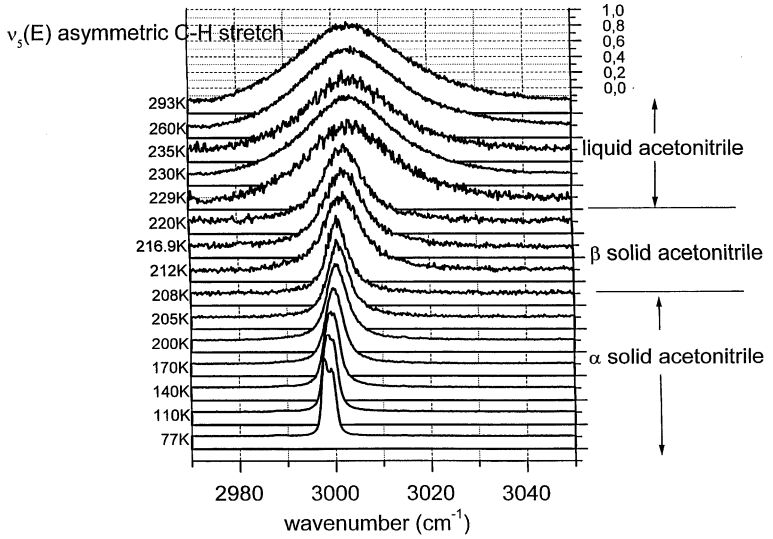

Fig. 1. VV Raman spectra of the $\nu_5(E)$ asymmetric C–H stretching mode of acetonitrile as a function of temperature.

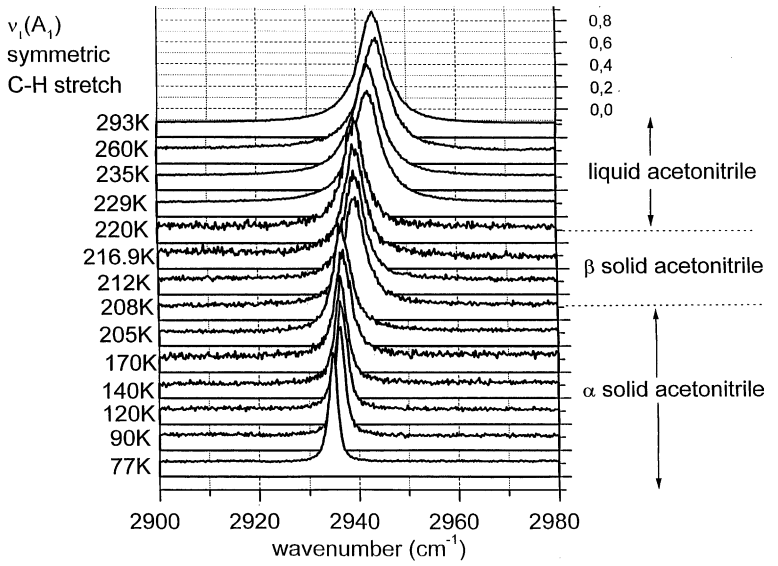

Fig. 2. VV Raman spectra of the $\nu_1(A_1)$ symmetric C–H stretching mode of acetonitrile as a function of temperature.

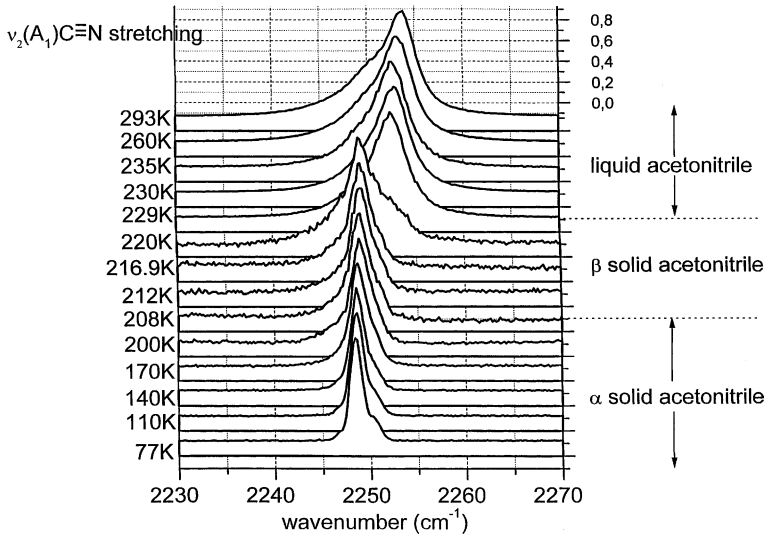

Fig. 3. VV Raman spectra of the $\nu_2(A_1)$ symmetric C≡N stretching mode of acetonitrile as a function of temperature.

229 K and some bands split into a maximum of three components. Careful examination of the results from Figs. 1–7 shows evidently that in all cases we can distinguish three different regions of spectral behaviour with the sudden, apparently discontinuous changes in the bandwidths, band shapes and maximum peak positions. The first region is between 293 and 229 K, the second one between 229 and 208–212 K for CH_3CN (and 216.9 K for CD_3CN not shown in Figs. 1–7), and the third one below those temperatures. As the temperatures correspond closely to the temperatures of the liquid–β acetonitrile, and $\beta \rightarrow \alpha$ transitions reported in the literature [25,26,30] and

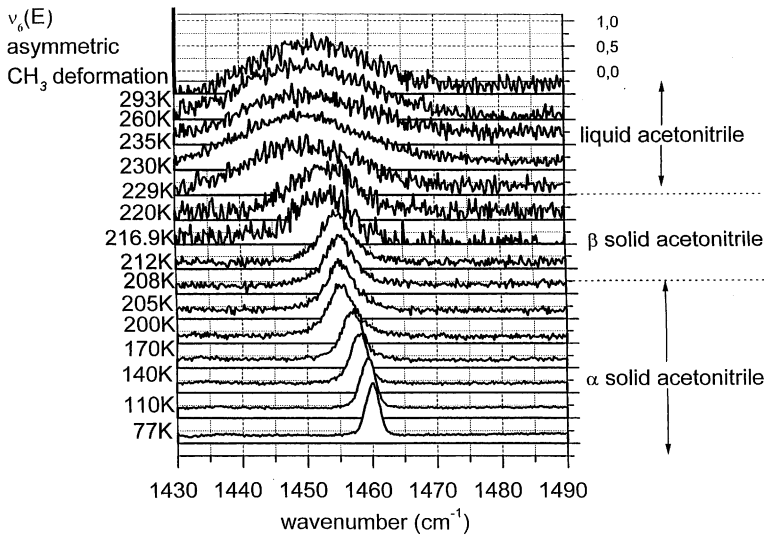

Fig. 4. VV Raman spectra of the ν_6(E) asymmetric CH_3 deformation mode of acetonitrile as a function of temperature.

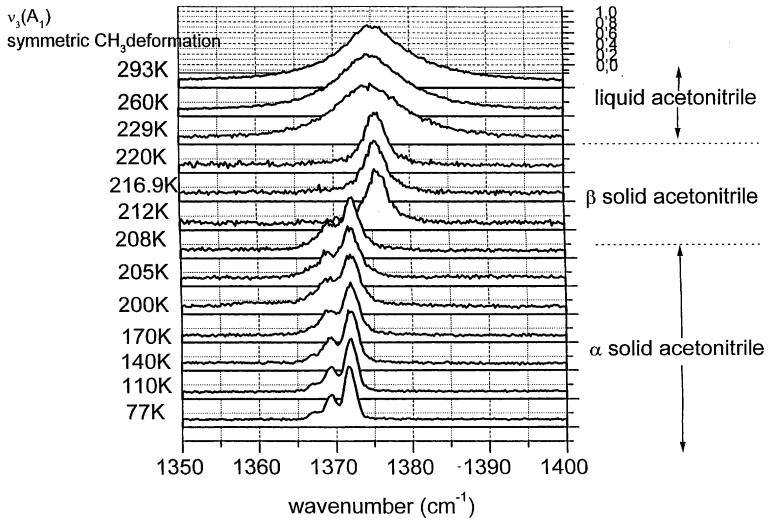

Fig. 5. VV Raman spectra of the $\nu_3(A_1)$ symmetric CH_3 deformation mode of acetonitrile as a function of temperature.

those obtained from our DSC measurements, we assigned the regions to liquid acetonitrile, β solid acetonitrile, and α solid acetonitrile, respectively. The temperature of 208–212 K for the $\beta \rightarrow \alpha$ transition obtained from our Raman and DSC results seems to be a little lower than obtained previously [26,30] for CH_3CN and agree very well with the reported 216.9 K for CD_3CN.

The molecular oscillators are particularly sensitive to the environment, and the sudden change in the band shapes and peak positions shown in Figs. 1–7 must reflect the structural reorganisation that occurs during the phase transitions. The detailed mechanisms of vibrational dephasing and vibrational energy relaxation leading to the changes of the band shapes and bandwidths will be discussed

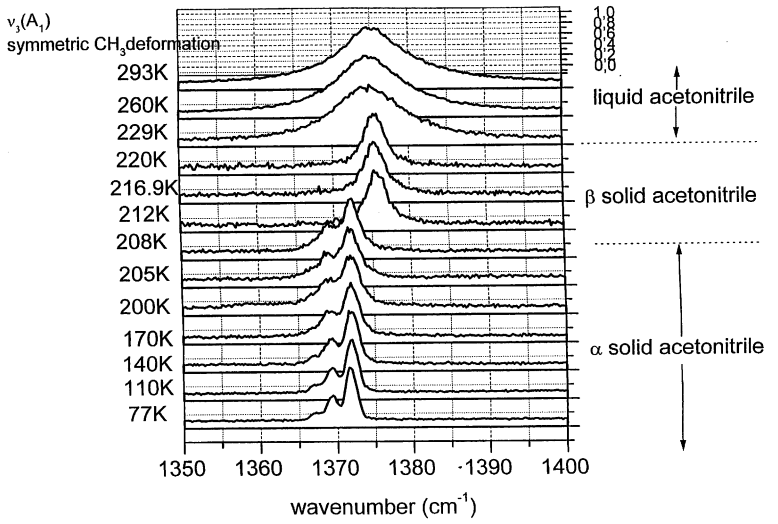

Fig. 6. VV Raman spectra of the $\nu_4(A_1)$ symmetric C–C stretching mode of acetonitrile as a function of temperature.

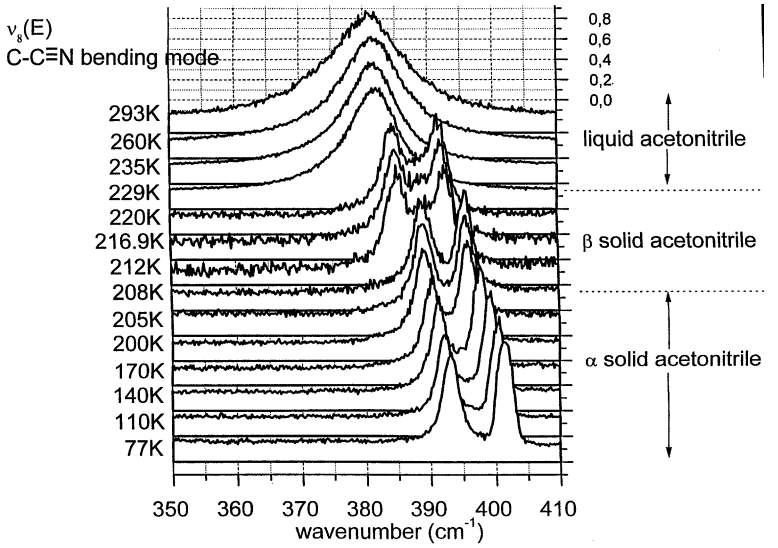

Fig. 7. VV Raman spectra of the $\nu_8(E)$ C–C≡N bending mode of acetonitrile as a function of temperature.

in a subsequent paper. Here, the main goal of the presentation and discussion will concentrate on the static vibrational properties of acetonitrile.

First, we need to ask for the origin of the splitting observed for the fundamentals of acetonitrile showed in Figs. 1–7. In general, the splitting may depend on the following factors:

1. a factor group splitting of the crystal [33],
2. a site group splitting caused by the reduction of molecular symmetry, which leads to removing the degeneracy of the vibrations [33],
3. coexistence between monomers and dimers or clusters containing larger number of acetonitrile molecules,

4. splitting due to tunnelling through periodic barrier for internal rotations of the methyl group,
5. shift of vibrational components of the fundamentals of acetonitrile due to the coupling with translational and librational lattice external vibrations,
6. splitting due to the hot librational transitions of the methyl group of acetonitrile.

It was found [28] that the tunnelling splitting are 1.5×10^{-5} and 5.47×10^{-4} cm^{-1} for both α and β phases, are far below the Raman spectroscopy resolution limit and it is clear that the tunnelling through periodic barrier for motion of the CH_3 group can be neglected as a reason of splitting observed in the Raman spectra.

Experimentally observed splitting of 8.37 cm^{-1} for the $\nu_8(E)$ mode of acetonitrile corresponds roughly to the energy of $2B$, where B is the rotational constant for the rotation around the C_3 molecular axis of acetonitrile and is equal to 5.56 cm^{-1} in the gas phase [34]. It may suggest that the origin of the splitting comes from the hot transitions for the internal librations of the methyl group in the lattice. Moreover, comparing the splitting obtained in this work for the $\nu_8(E)$ mode of CH_3CN (8.37 cm^{-1}) and of CD_3CN (6.86 cm^{-1}) one can notice that the ratio of $8.37/6.86 = 1.22$ corresponds roughly to the ratio of $(I^D/I^H)^{1/2} = 1.41$ predicted for the librational motion of the methyl group under isotopic substitution, where I^D and I^H are the moments of inertia for deuterated and nondeuterated species, respectively. However, taking into account that the β and α phases of acetonitrile are stable and undergo the equilibrium Boltzmann population, we can calculate that the librational transitions involving the higher quantum numbers should contribute much less effectively at 77 K, which is in contrast to the experimental spectra (Fig. 7) with approximately the same intensities for both components of the $\nu_8(E)$ mode. Thus, the hot transitions for the libration around the C_3 molecular axis of acetonitrile as a reason of splitting can be ruled out.

However, it is interesting to notice (Fig. 8a and b) that the band of the $\nu_8(E)$ mode at 220 K has three components, in contrast to two components at 77 K. This additional peak at 388.56 cm^{-1} is likely to correspond to a large-amplitude librational transitions from the higher states ($J > 0$). The splitting into three components at 220 K: 384.38, 388.56, and 391.64 cm^{-1} gives energy of around 4 cm^{-1} that is much lower than $2B$ for the libration of the methyl group around the C_3 axis. It corresponds much better to the motion characterised by the rotational constant B around the axis perpendicular to the C_3 axis [34]. This finding suggests that the β phase has a relatively large degree of reorientational or librational freedom around the axis perpendicular to the molecular axis C_3 (Fig. 8a), in contrast to the α phase where this kind of motion is frozen at 77 K (Fig. 8b). The results presented in Fig. 8 seem to support the mechanisms proposed for the $\beta \rightarrow \alpha$ transition in Ref. [26]. The authors suggested that the $\beta \rightarrow \alpha$ transition is accompanied by change of the orientation of the permanent dipoles of acetonitrile molecules that lead to a structure with a macroscopic polarisation in the c direction and parallel alignment of the dipoles in the α phase, in contrast to the anti-parallel alignment for the β phase. In order such a reorganisation could take place the reorientations must involve a change by 90° the orientation of the molecular C_3 axis of four molecules in the unit cell.

To learn more about the origin of the splitting mentioned above we have performed studies on the changes in band shapes upon isotopic substitution. The isotopic mixtures studies are very effective in determining the nature of the splitting in crystals as the multiplet structure of nonsubstituted crystal should be perturbed severely in isotopic mixtures if the factor group splitting plays a crucial role. The first order solution of the perturbation theory for the frequency of the αth component of the multiplet associated with ith nondeuterated vibration of the free molecule is

$$h\nu_{i,\alpha} = h\nu_i^0 + M^{i\alpha} \tag{1}$$

where $M^{i\alpha}$ depends on [36,37]

$$\sum B^*_{\alpha r} B_{\alpha q} \int \left(\Psi^i_u \Psi^0_v\right)^* V_{uv} \left(\Psi^0_\alpha \Psi^i_v\right) \mathrm{d}\tau \tag{2}$$

and represents a splitting term. It has a different value for each wave vector $\vec{q} = 0$ component in the

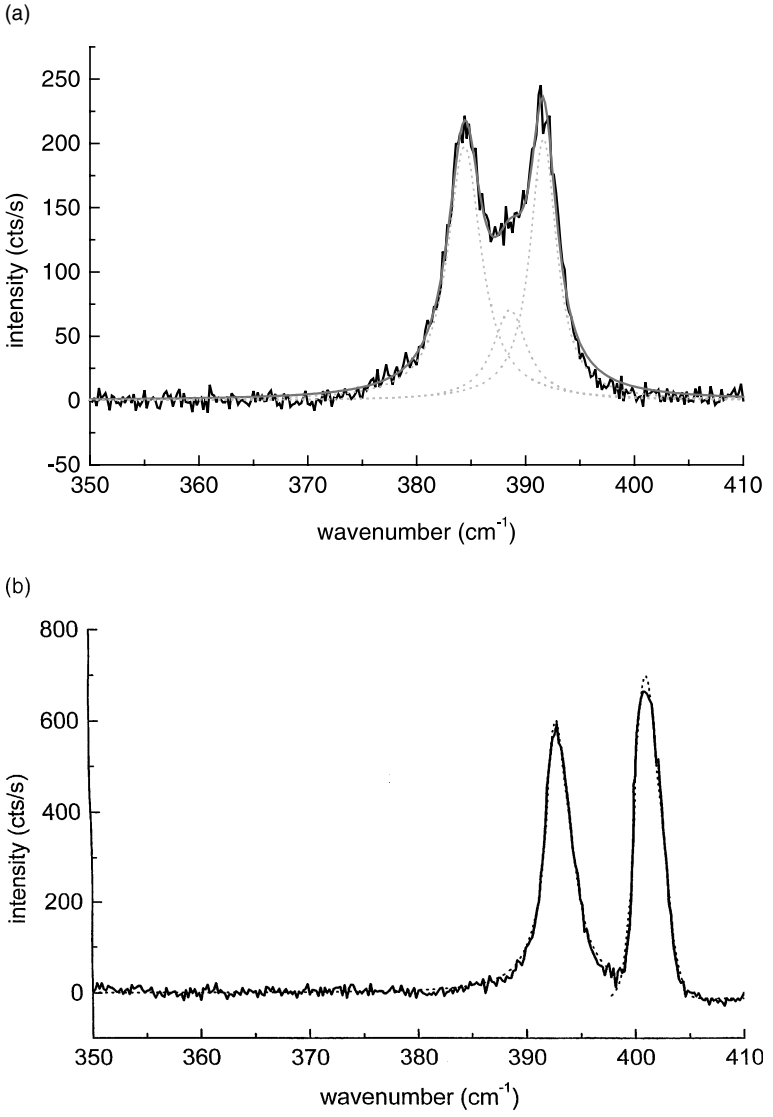

Fig. 8. VV Raman spectra of the C–C≡N bending mode of acetonitrile as at: (a) 220 K: fitting of experimental data with three Lorentz components, and (b) 77 K: fitting of the experimental data with one Lorentz and one Gaussian components.

crystal exciton band. $V_{u,v}$ is the intermolecular potential between the molecules u and v, Ψ_u^i, Ψ_v^i, Ψ_v^0, Ψ_α^0 represent the wave function of the ith vibration for the u molecules (on sites r) and v molecules (on sites q) for the ground (0) and excited states (i). If there are Z molecules in the unit cell, each vibrational mode will split into Z components and this effect is known in the literature as the factor group splitting or Davydov splitting. As the number of identical oscillators Z in the unit cell is modified with the isotopic dilution the splitting that comes from the resonance interactions V_{uv} must change. When the isotopic dilution is sufficiently large to remove the resonance interaction, the multiplet structure should disappear and a single peak should be observed.

As an example we show in Fig. 9a–c the effect of isotopic dilution for the doubly degenerated mode

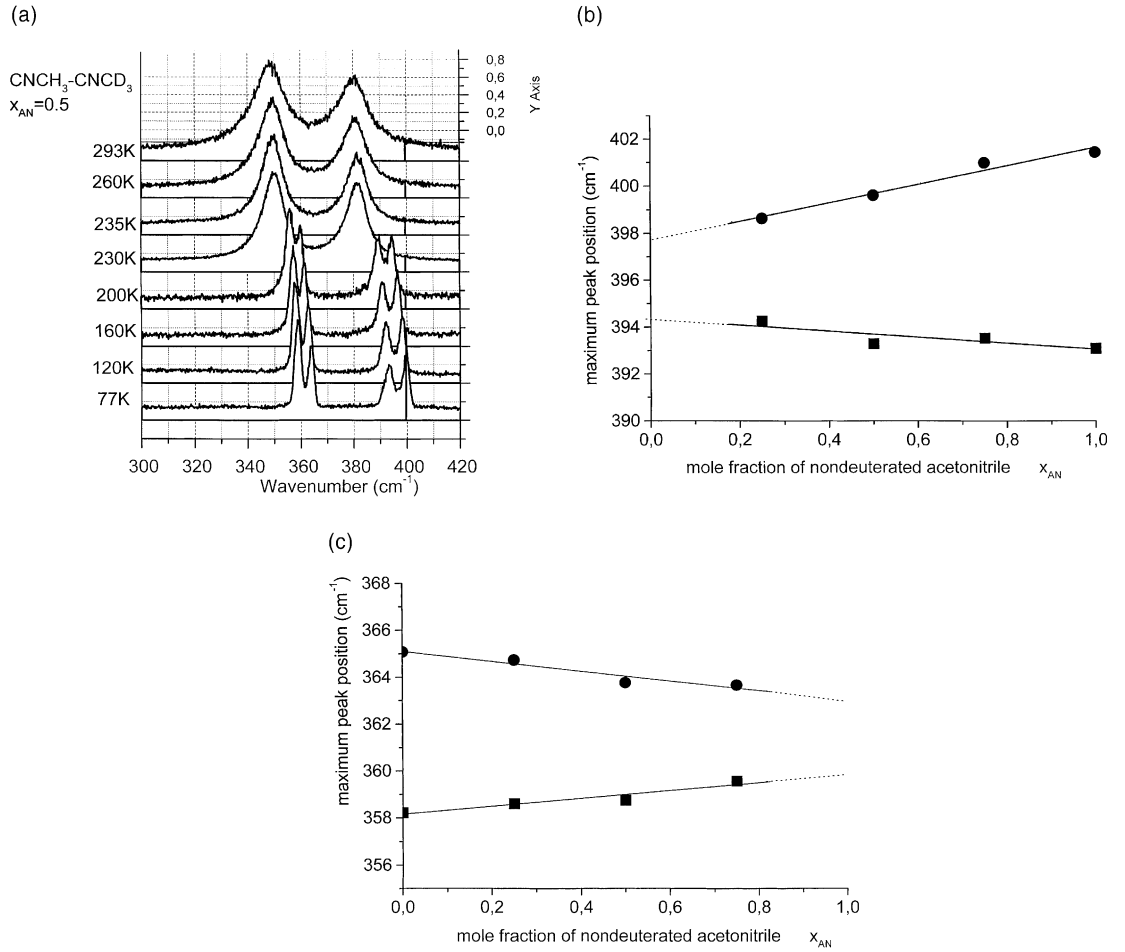

Fig. 9. (a) VV Raman spectra of the ν_8(E) C–C≡N bending mode of deuterated acetonitrile and acetonitrile as a function of temperature in the isotopic mixture $CNCH_3$–$CNCD_3$ ($X_{AN} = 0.5$); Maximum peak positions of the C–C≡N bending mode ν_8 of acetonitrile in the isotopic mixture $CNCH_3$–$CNCD_3$ as a function of the mole fraction of nondeuterated acetonitrile X_{AN}, (b) ν_8 mode of $CNCH_3$, (c) ν_8 mode of $CNCD_3$, (■,●) Raman experimental data.

ν_8(E). It is clear from Fig. 9b and c that the magnitude of the splitting becomes significantly smaller with isotopic dilution. Unfortunately, it is not possible to reach very low concentrations in the isotopic mixtures with Raman spectroscopy because the signals become very weak with dilution. The results presented in Fig. 9a–c compared with the results from Fig. 5 answer the question if the splitting is produced by the factor group splitting or by the site group splitting due to the reduction of the molecular symmetry as the direct result of the surrounding crystalline field. The splitting of the A_1 symmetry fundamental $\nu_3(A_1)$ observed in Fig. 5 must arise from the factor group splitting, because the site group splitting is absent for the totally symmetric modes. The site group splitting may lead to further splitting of the doubly degenerate modes, which is not observed for the ν_5(E) (Fig. 1) and the ν_8(E) modes (Fig. 7). It clearly indicates that the splitting of all the vibrational modes of acetonitrile must come from the factor group splitting. Moreover, the isotopic substitution effect for the E symmetry mode ν_8(E) from Fig. 9b and c provides an additional support

that the factor group splitting must be responsible for the multiplet features of the Raman spectra of acetonitrile both for the symmetric and the degenerate modes. Indeed, the site splitting at the site cannot be the origin of the splitting in solid acetonitrile, because the degeneracy of the vibrations removed in the crystal would be the same in the deuterated and nondeuterated crystals due to commonly assumed isostructural properties for both species. As a consequence there should be no change with isotopic composition in contrast to the experimental results in Fig. 9b and c.

The conclusion that the splitting of the vibrational modes of acetonitrile must come from the factor group splitting combined with the results of Figs. 1–7 clearly indicate the presence of at least three molecules per unit cell both for β and α phases. The crystallographic studies showed that there are four molecules in the unit cell ($Z = 4$) for both β and α phases [20,21,24–27]. The results from Figs. 1–7 lend no support to the conclusion that there is a change in the number Z from four to eight at the $\beta \rightarrow \alpha$ transition suggested in Ref. [19] as the change in the number Z should be accompanied by marked increase in the number of components in the multiplet structure of the vibrational bands, which is not observed in the spectra presented here.

Comparison between the multiplet structure of the IR and Raman spectra that are presented in Table 1 may provide information about the symmetry site. If the Raman-IR noncoincidence (the rule of mutual exclusion) occurs, it will supports strongly the existence of the symmetry centre at the site. Table 1 shows clearly the lack of coincidence in the IR and Raman multiplet structure for some vibrational modes both for α acetonitrile at 77 K. Similar lack of coincidence is observed for β acetonitrile at 220 K (not shown in Table 1). It would suggest that both α and β phases possess a symmetry centre with the neighbouring molecules having an anti-parallel alignment which is in contrast with the conclusions obtained from the crystallographic data. The crystallographic structure proposed for the β phase [24] belongs to the monoclinic space group $P2_1/c$ and possesses the symmetry centre, while the α phase was obtained to have the orthorhombic $Cmc2_1$ space group [25,26,31] and does not possess the symmetry centre. Although vibrational spectroscopy may help in structure determination, but we should be very careful when we compare the multiplet structure from IR and Raman spectra taken from different sources. First of all, not all IR and Raman features like splitting of vibrational fundamentals that appear when the sample is cooled can be correctly associated with the crystal symmetry. Some bands may arise from thermally populated

Table 1

α (cm^{-1})			Symmetry assignment
81.15 K [19]	Raman 77 K (VV) This work	Raman 80 K [20]	
–	–	–	$\nu_5(E)$
–	2999.4	2997	
2995.7	2997.7	2996	
–	–	–	$\nu_1(A_1)$
–	2936.3	2936	
2933.2	–	2933	
1457	1460	1458	
1456.2	–	–	
1452.1	–	–	$\nu_7 + \nu_8(A_1 + A_2 + E)$ [20] $\nu_3 + T_{xy}$
–	–	–	
1436.1		1437	
1425.4		1426	
1421.4		–	$\nu_6 + \nu_7 + \nu_8$ [20]
1419.4		–	
			$\nu_6(E)$ [32]
2247.3	2250.3	2247	$\nu_2(A_1)$
–	2248.4	2246	
–	–	–	$\nu_3(A_1)$
1370.1	1371.6	1370	
1367.9	1369.0	1367	
1365.9	1366.7	1366	
1043.3		1047	$\nu_7(E)$
1039.4		1042	
1034.2		1038	
920.5	921	921	$\nu_4(A_1)$
919.0	–	–	
915.4	915.4	–	
400.5	402.0	400	$\nu_8(E)$
396.5	–	–	
391.7	–	391.7	
–	393.89	–	

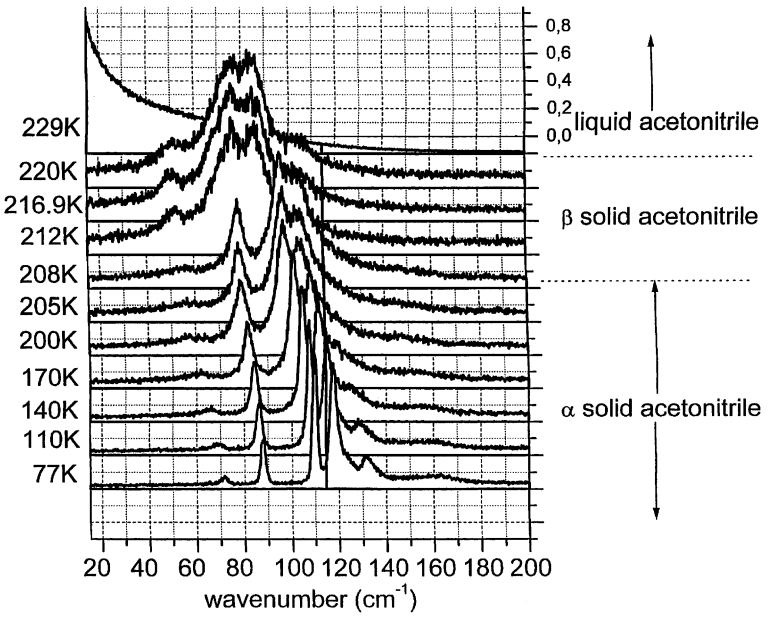

Fig. 10. Raman spectra of the lattice region 15–200 cm^{-1} for acetonitrile as a function of temperature.

rotational states. Moreover, at higher temperatures (in this case above 216.9 K) the thermally activated mechanisms of vibrational dephasing lead to band broadening and vibrational structure may not longer be resolvable, which results in the apparent change of the number of components. In some cases the extended structure of acetonitrile may appear in cases of incomplete conversion of the β form into the α form during the solid–solid phase transition.

Fortunately, one of the greatest advantages of Raman spectroscopy is that it can provide information about the external vibrational modes that are particularly sensitive to crystalline effects. They may help to illustrate the change that occurs at the liquid–β solid acetonitrile at 229 K and β solid–α solid transitions at around 208–212 K.

Fig. 10 shows the Raman spectra of CH_3CN in the lattice region 15–200 cm^{-1} (in the region from 200 to the $\nu_8(E)$ bending mode at around 380 cm^{-1} we do not observe any peaks) as a function of temperature. The rather dramatic and sudden changes in the line shapes, widths, and peak positions with temperature in the lattice region shown in Fig. 10 must reflect obviously structural reorganisations due to the phase transitions. At 229 K corresponding to the liquid–β acetonitrile transition where the solidification starts we still observe the Rayleigh–Brillouin scattering wing without any solid lattice structure. Shortly below this temperature the crystal structure of the β phase begin to appear. The translational and rotational degrees of freedom: $T_z(A_1)$, $L_z(A_2)$, $T_{xy}(E)$, $R_{xy}(E)$ of acetonitrile belonging in the liquid phase to the point group C_{3v} become the translational and librational optical lattice modes oscillating out of phase in the crystal unit cells. In the β phase (between 229 and 212–208 K) the lattice vibrations are not well resolved due to the thermally activated dephasing of the external modes. As we can see from Fig. 10 the bands of the β phase are very broad and it may indicate a plastic structure with rotational disorder of the CH_3 group. At the temperature corresponding to the $\beta \rightarrow \alpha$ transition at around 212–208 K (CH_3CN) (and 216.9 K for CD_3CN not shown here) one can see the remarkable, sudden blue shift of about 20–40 cm^{-1} depending on the vibrational mode. With temperature decreasing the bands become more and more narrow and we observe the further gradual blue shift of the α stable phase of acetonitrile until 77 K. Anderson and Zeng [38] found that the

Raman and far-infrared spectra of the low temperature α phase are simpler than those of the upper phase which is obviously not supported by our data.

To learn more from the Raman lattice spectra a few remarks explaining the origin of the external modes may be appropriate. In Table 2 we have shown the Raman spectra of the lattice region 15–200 cm^{-1} mode. The results are compared with those obtained previously [20,23,28]. The maximum peak positions for the stable α phase of acetonitrile obtained in this paper agree very well with those obtained in Ref. [20] whereas large discrepancies are observed when compared with the results of Ref. [28]. The most significant difference in the Raman and INS assignments illustrated in Table 2 occurs around 202 cm^{-1} where INS method shows a strong peak of the methyl group [28], which is not observed in the Raman spectra. As the inelastic neutron scattering (INS) used in Ref. [28] cannot compete with vibrational spectroscopy resolutions in the frequency domain we believe that the deviations come from the different resolutions of the two techniques. Table 2 shows the assignment of the lattice modes based on the ratios R of the deuterated and nondeuterated species peak positions and compared with the magnitudes of $(M^{D}/M^{H})^{1/2} = 1.036$ (predicted for the translational vibrations), $(I_{A}^{D}/I_{A}^{H})^{1/2} = 1.41$ and $(I_{B}^{D}/I_{B}^{H})^{1/2} = 1.082$ (predicted for the librational vibrations parallel and perpendicular to the molecular C_3 axis of acetonitrile, respectively). These theoretical numbers are exact only for the case when the C_3 axis is directed along the crystallographic c axis, which does not seem to happen [21,24,26] for acetonitrile. We can see from Table 2 that the ratio of 1.41 was never reached indicating that there is no evidence of the $L_z(A_2)$ librational vibration of the CH_3 group around the C_3 axis in the α phase. The peak at 202 cm^{-1} assigned to $L_z(A_2)$ by INS method [28] is not observed in the Raman spectra. It clearly indicates that the internal rotation of the CH_3 group in the α phase is frozen.

The results obtained for the external vibrations are very encouraging, and suggest that abrupt structure reorganisation occurs at the $\beta \rightarrow \alpha$ acetonitrile transitions. In order to illustrate this point and further expose the nature of structural changes occurring during the phase transitions of acetonitrile we will focus on the internal modes. The modification of the transition frequencies for internal vibrations of molecules in condensed phases is the result the competition between the repulsive (blue shift) and attractive (red shift) interactions. Numerous theoretical approaches have been proposed [8,35] to understand the short-range repulsive and long-range attractive interac-

Table 2

α acetonitrile						
This work 77 K			Ref. [20] 80 K			Ref. [28] 20 K
CH_3CN (cm^{-1})	CD_3CN (cm^{-1})	R	CH_3CN (cm^{-1})	CD_3CN (cm^{-1})	R	CH_3CN (cm^{-1})
–	–	–	–	–	–	50
65	–	–	–	–	–	–
68	70	$0.971T_{xy}$(E)	69	69	$1.000T_{xy}$ (E)	77
86	86	$1.000T_{xy}$(E)	87	84	$1.036T_{xy}$(E)	$85T_{xy}$(E)
–	–	–	–	–	–	94
108	102	$1.058L_{xy}$(E)	109	101	$1.079T_{xy}$(E)	103
117	107	$1.093L_{xy}$(E)	117	107	$1.093L_{xy}$(E)	–
121	110	$1.100L_{xy}$(E)	121	110	$1.000L_{xy}$(E)	–
131	124	$1.056L_{xy}$(E)	131	122	$1.074L_{xy}$(E)	$125T_z(A_1)$
136	–	–	134	–	–	$136L_{xy}$(E)
–	145	–	145	144	$1.007T_z(A_1)$	–
–	–	–	152	–	–	–
160	160	$1.000T_z(A_1)$	159	156	$1.019T_z(A_1)$	–
	–	–	–	–	–	$202L_z(A_2)$

tions on vibrational frequency shift. Unfortunately, most of them cannot be applied to solids as they assume a liquid-like pair distribution function and the long-range attractive dipole interactions are angle averaged.

The failure of the existing theoretical models in detail reproduction of the experimental data for the solid phases does not imply that it is totally obscure what features of the intermolecular interactions make the oscillator behave the way illustrated in the Raman spectra. Careful examination of the vibrational frequency shifts around the phase transitions temperatures illustrated in Figs. 1–7 provides qualitative information on molecular mechanisms occurring at the phase transitions.

The sudden vibrational shift due to repulsive forces is associated only with a discontinuous change in volume (and density) due to close packing at the phase transition as it is predicted from the hard-sphere models [8]. In contrast, the discontinuous vibrational shift at the phase transition due to attractive forces may depend both on discontinuity in density and the discontinuous change in the nature of interactions between the molecules due to sudden structure reorganisation. In this context, it is very valuable when confronting the results in Figs. 3 and 5. The ν_2 (C≡N) stretching vibration in Fig. 3 displays the sudden red shift at the liquid–β solid transition of acetonitrile and no further changes at the $\beta \rightarrow \alpha$ transition are observed. In contrast, the deformation vibration of the methyl group $\nu_3(A_1)$ displays no changes at liquid–β solid transition (Fig. 5), but significant sharp shift at the $\beta \rightarrow \alpha$ transition. The other vibrations of the methyl group as well as the bending mode C–C≡N $\nu_8(E)$ (Figs. 7 and 9) are sensitive to both transitions. It is clear that the discontinuous density shift should influence both vibrations in Figs. 3 and 5 in the similar way, although the magnitudes of the vibrational shifts are generally different for various vibrations. The mechanisms underlying the features of the frequency shifts in Figs. 3 and 5 can be qualitatively understood only if we assume that the density effects are strongly modified by the sudden changes in the nature of interactions between the molecules in the first coordination shell around the oscillators at the $\beta \rightarrow \alpha$ transition. Indeed, the sharp red shift observed in Fig. 3 for the C≡N stretching mode at the liquid–β solid transition temperature reflects stronger than in liquid phase attractive interactions due to the ordering of the anti-parallel aligned dipoles in the β solid phase. The $\nu_3(A_1)$ CH_3 deformation mode is not so sensitive to the dipole–dipole interactions and the ordering of the C≡N dipoles does not play such an important role because of rotational disorder of the CH_3 group. As a consequence the ordering of the C≡N dipoles does not contribute so much to the shift at the liquid–β solid transition temperature for the $\nu_3(A_1)$ CH_3 deformation mode in Fig. 5. Thus, the sudden red shift observed for the ν_3 mode in Fig. 5 at the β solid $\rightarrow \alpha$ solid transition temperature must reflect the attractive interactions due to density increase rather than further ordering of dipoles. However, the similar changes should be expected for the C≡N stretching mode at the $\beta \rightarrow \alpha$ transition temperature, but it is certainly not supported by the experimental shift in Fig. 3. The lack of the red frequency shift at the $\beta \rightarrow \alpha$ transition for the C≡N stretching mode indicates that the attractive shift due to density effect must be balanced by decrease in the magnitude of attractive dispersive and dipole–dipole interactions. Otherwise, the more pronounced red shift at the $\beta \rightarrow \alpha$ transition should be observed for ν_2, not ν_3, in contrast to the experimental results in Figs. 3 and 5. The decrease in the magnitude of attractive interactions must reflect the change in the nature of the attractive interactions. It cannot be associated with the changes due to the further increasing of anti-parallel ordering of the dipoles, because this kind of interactions would lead to the further red shift for the C≡N stretching mode, in contrast to the experimental data in Fig. 3. On the contrary, it must reflect the changes in the orientation of molecular dipoles from anti-parallel alignment to parallel alignment. Thus, the only reasonable explanation is that the vibrational shifts in Figs. 3 and 5 illustrate the change in the nature of the attractive interaction from anti-parallel in the β phase to parallel in the α phase. This conclusion is in reasonable agreement with that proposed by Antson and Tilli [26] and Torrie and Powell [31] for the structure of the β and α phases of acetonitrile on the basis of crystallographic investigations.

Their results suggested dramatic changes in the orientation of permanent dipoles of the acetonitrile molecules, which lead to a structure of α acetonitrile with a macroscopic polarisation along of the crystallographic axis *c*.

4. Conclusions

Based on the Raman spectroscopic results reported here, we can make the following general observations concerning the correlation between the phase transitions in acetonitrile and interactions between the molecular oscillator and the surrounding molecules.

All the vibrational modes of acetonitrile are very sensitive to the structural changes that occur at the liquid–β solid and β solid–α solid transitions. The only exception is the C–C stretching mode that displays the smallest changes. The vibrational frequency shifts of all the modes of acetonitrile display apparently discontinuous changes at the phase transitions.

The mechanisms underlying these features can be qualitatively understood if we assume that the behaviour of vibrational degrees of freedom at the phase transitions is associated not only with a discontinuous change in volume but also sudden changes of entropy. The discontinuous change in volume influences strongly the repulsive forces around the oscillator and that part of attractive contribution that depends linearly on density (a van der Waals mean field interaction) whereas the discontinuous entropy changes reflect the ordering due to strongly anisotropic part of the attractive potential of acetonitrile. Molecular mechanism governing both phase transitions, from liquid to β solid and from solid β to solid α, lead to significant reorganisation of the structure. Key characteristics of the molecular dynamics leading to structural reorganisation at both phase transitions is that they involve reorientational or librational motions around the axis perpendicular to the C_3 molecular axis. The results presented in this paper show that this kind of motions is relatively free in the β solid phase and it becomes to be frozen at around 90 K.

The most important structural change occurs at the solid β–solid α transition. Our results support the conclusion obtained from the recent crystallographic data [26] that the $\beta \rightarrow \alpha$ transitions is accompanied by a drastic change in the orientation of the molecular dipole moments from an antiparallel alignment for the neighbouring molecules in the β phase to a parallel alignment in the α phase. Such a large angle reorientation of acetonitrile molecule is possible in the β phase where the crystal structure is not fully formed and it exhibits a large degree of plasticity. This feature is clearly demonstrated by results presented in this paper for the Raman lattice vibrations between 229 and 208 K that are indicative of a large degree of reorientational disorder of the CH_3 group.

Careful examination of the behaviour of the oscillators with decreasing temperature, with a special emphasis on the phase transition temperatures, leads to the conclusion that the structural reorganisation at the $\beta \rightarrow \alpha$ transition results in stronger attractive interactions between C–H and nitrogen and/or weaker repulsive interactions between the methyl groups of the neighbouring molecules. Furthermore, the attractive interactions between the permanent dipoles become weaker below the $\beta \rightarrow \alpha$ transition temperature and illustrate the change in the orientations of the molecular dipoles from an anti-parallel to a parallel alignment in the α solid acetonitrile.

The isotopic substitution effect on the Raman spectra makes clear that the origin of splitting in solid acetonitrile comes from the factor group splitting, not the site group splitting. The other possible factors that may lead to multiplet structure of solid acetonitrile have been ruled out.

In this paper we have confined ourselves mainly to the results for the stable, equilibrium structure of acetonitrile. However, we have also monitored Raman spectra for the metastable, nonequilibrium structure called here supercooled β acetonitrile, which will be presented in the subsequent paper. We hope that comparing the results for the stable and metastable phases may provide deeper understanding of the mechanisms that occurs during the phase transitions. We hope the results presented here will help to obtain a more illuminating picture elucidating which degrees of freedom melt at the transition from the disordered, isotropic structure of liquid phase to partially ordered β

structure and fully ordered α crystal structure of solid acetonitrile.

Acknowledgements

We thank Professor B. Ladanyi from Colorado State University for several useful discussions. The authors gratefully acknowledge the support of this work by the Polish-American grant of M. Skłodowska-Curie Fund II and Foundation for Polish Science. Support from the Dz.S. 2001 is also acknowledged.

References

[1] I. Nakagawa, T. Shimanouchi, Spectrochim. Acta 18 (1962) 513.
[2] R. Yamadera, S. Krimm, Spectrochim. Acta A 24 (1968) 1677.
[3] P.O. Westlund, R.M. Lynden-Bell, Mol. Phys. 60 (1987) 1189.
[4] J. Yarwood, R. Arndt, G. Doge, Chem. Phys. 25 (1977) 387.
[5] H. Beretagnolli, M.D. Zeidler, Mol. Phys. 35 (1978) 177.
[6] K. Tanabe, Chem. Phys. 38 (1979) 125.
[7] C. Breuillard-Alliot, J. Soussen-Jacob, Mol. Phys. 28 (1974) 905.
[8] D. Ben-Amotz, M.R. Lee, S.Y. Cho, D.J. List, J. Chem. Phys. 96 (1992) 8781.
[9] M. Maroncelli, J. Chem. Phys. 94 (1990) 2084.
[10] S.M. George, A.L. Harris, M. Berg, C.B. Harris, J. Chem. Phys. 80 (1984) 83.
[11] D. McMorrow, W.T. Lotshow, J. Phys. Chem. 95 (1991) 10395.
[12] P. Yuan, M. Schwartz, J. Chem. Soc. Faraday Trans. 86 (1990) 593.
[13] L.J. Muller, D. Vanden Bout, M. Berg, J. Chem. Phys. 99 (1993) 810.
[14] B.M. Ladanyi, R.M. Stratt, J. Phys. Chem. A 102 (1998) 1068.
[15] J.C. Deak, L.K. Iwaki, D.D. Dlott, J. Phys. Chem. 102 (1998) 8193.
[16] W. Kunz, P. Calmettes, M.C. Bellissent-Funel, J. Chem. Phys. 99 (1993) 2079.
[17] G. Del Mistro, A.J. Stace, J. Chem. Phys. 99 (1993) 4656.
[18] A.J. Stace, G. Del Mistro, J. Chem. Phys. 102 (1995) 5900.
[19] E.L. Pace, L.J. Noe, J. Chem. Phys. 49 (1968) 5317.
[20] M.P. Marzocchi, M.G. Migliorini, Spectochim. Acta 29A (1973) 1643.
[21] M.P. Marzocchi, S. Dobros, Spectochim. Acta 30A (1974) 1437.
[22] A. Kaplan, A. Gattoni, J. Mol. Sruct. 58 (1980) 283.
[23] E. Knozinger, D. Leufloff, J. Chem. Phys. 74 (1981) 4812.
[24] M.J. Barrow, Acta Cryst. B 37 (1981) 2239.
[25] S.F. Trevino, C.S. Choi, J. Chem. Phys. 98 (1993) 78.
[26] O.K. Anston, K.J. Tilli, Acta Cryst. B 34 (1987) 296.
[27] F.R. Trouw, J.W. White, J. Chem. Soc. Faraday Trans. 84 (1988) 813.
[28] P.H. Gamien, W.J. Stead, J. Tomkinson, J.W. White, J. Chem. Soc. Faraday Trans. 87 (1991) 539.
[29] W.E. Putnam, D.M. McEarchen Jr., J.E. Kilpatrick, J. Chem. Phys. 42 (1965) 749.
[30] P.A. Casabella, P.J. Bray, J. Chem. Phys. 32 (1960) 314.
[31] B.H. Torrie, B.M. Powell, Mol. Phys. 75 (1992) 613.
[32] J.C. Evans, H.J. Bernstein, Cand. J. Chem. 33 (1956) 1746.
[33] G. Turrell, Infrared and Raman Spectra of Crystals, Academic Press, New York, 1972.
[34] P.S. Goyal, J. Pendolf, J. Ttomkinson, Chem. Phys. Lett. 127 (1986) 483.
[35] K.S. Schweizer, D. Chandler, J. Chem. Phys. 76 (1982) 2296.
[36] R. Kopelman, J. Chem. Phys. 47 (1967) 2631.
[37] R.M. Hexter, J. Chem. Phys. 36 (1962) 2285.
[38] A. Anderson, W.Y. Zeng, J. Raman Spectrosc. 17 (1986) 447.